Journal Name

ARTICLE

The effect of solvent relaxation in the ultrafast time-resolved spectroscopy of solvated benzophenone.†

Received 00th January 20xx,
Accepted 00th January 20xx

DOI: 10.1039/x0xx00000x

www.rsc.org/

Elena Zvereva,[a,b,c] Javier Segarra-Martí,[d*] Marco Marazzi,[a,b*] Johanna Brazard,[e] Artur Nenov,[f] Oliver Weingart,[g] Jérémie Léonard,[e] Marco Garavelli,[f] Ivan Rivalta,[d] Elise Dumont,[d] Xavier Assfeld,[a,b] Stefan Haacke,[e] and Antonio Monari[a,b*]

Benzophenone (BP) despite its relatively simple molecular structure is a paradigmatic sensitizer, featuring both photocatalytic and photobiological effects due to its rather complex photophysical properties. In this contribution we report an original theoretical approach to model realistic, ultra-fast spectroscopy data, which requires describing intra- and intermolecular energy and structural relaxation. In particular we explicitly simulate time-resolved pump-probe spectra using a combination of state-of-the art hybrid quantum mechanics/ molecular mechanics dynamics to treat relaxation and vibrational effects. The comparison with experimental transient absorption data demonstrates the efficiency and accuracy of our approach. Furthermore the explicit inclusion of the solvent, water for simulation and methanol for experiment, allows us, despite the inherent different behavior of the two, to underline the role played by the H-bonding relaxation in the first hundreds of femtoseconds after optical excitations. Finally we predict for the first time the two-dimensional electronic spectrum (2DES) of BP taking into account vibrational effects and hence modelling partially symmetric and assymetric ultrafast broadening.

Introduction

Benzophenone (BP) is a well-known photosensitizer[1–4] and its photophysical and photochemical properties have been the subject of extended theoretical[5–7] and experimental studies.[1–3,8,9]

In particular, benzophenone is recognised for its efficient intersystem crossing that allows a quasi-unitary population of its triplet manifolds.[10–13] In turn this capacity has been exploited as a photo-catalytic initiator in many fields.[14,15] Furthermore benzophenone has also been recognised as a DNA photosensitizer[1,16,17] inducing a variety of phenomena including triplet-triplet energy transfer[18] and hydrogen abstraction.[19,20] Additionally, the widespread non-steroidal anti-inflammatory drug ketoprofen shares the same chemical core as BP and hence may open the same photosensitization pathways.[21–23]

Despite BP's simple chemical structure, the mechanism leading to intersystem crossing has been the object of an important scientific debate.[6,10,11] Recently, molecular modelling has explored the excited state landscape both from a static[6] and non-adiabatic dynamic point of views,[5,7] clearly underscoring the crucial role of the extended quasi-degeneracy between S_1, T_1 and T_2 state. Furthermore, a dynamic equilibrium between the two triplet states has also been predicted. Most interestingly, the aforementioned equilibrium enables not only T_1 population, but also a minor though significant population of the T_2 state up to the ps time scale,[5] that can in the following actively participate in the DNA photosensitization process via triplet-triplet energy transfer.[18]

For all these reasons, BP's importance goes far beyond practical applications and should also be regarded as a fundamental model system to explore complicate photochemical and photophysical phenomena, as well as photosensitization of both chemical and biological structures. In that respect the combined application of high-level molecular modelling and time-resolved spectroscopy should be considered as the strategy of choice to allow the precise unravelling of the electronic and structural bases of photophysical phenomena. In particular the possibility to efficiently and accurately model the excited states potential energy surface (PES) landscape remains a fundamental challenge in computational photophysics.[24]

[a] Université de Lorraine – Nancy, Laboratoire de Physique et Chimie Théoriques. Vandoeuvre-lès-Nancy, 54506 France
[b] CNRS, Laboratoire de Physique et Chimie Théoriques. Vandoeuvre-lès-Nancy, 54506 France
[c] A. E. Arbuzov Institute of Organic and Physical Chemistry, Kazan Scientific Centre, Russian Academy of Sciences, Arbuzov str. 8, 420088 Kazan, Russia
[d] Univ Lyon, Ens de Lyon, CNRS, Université Claude Bernard Lyon 1, Laboratoire de Chimie UMR 5182, F-69342, Lyon, France
[e] Université de Strasbourg, CNRS, Institut de Physique et Chimie des Matériaux de Strasbourg and Labex NIE, , 23 rue du Loess, 67034 Strasbourg Cedex, France.
[f] Università di Bologna, Dipartimento di Chimica Industriale "Toso Montanari" viale del Risorgimento 4, Bologna, Italy.
[g] Heinrich-Heine-Universität Düsseldorf, Institut für Theoretische Chemie und Computerchemie, Universitätsstr. 1, 40225 Düsseldorf, Germanyy
† A.M. Antonio.monari@univ-lorraine.fr, M.M. marco.marazzi@univ-lorraine.fr
J.S-M: Javier.segarra-marti@ens-lyon.fr
Electronic Supplementary Information (ESI) available: Computational details on the MD, DFT/MRCI and RASPT2. Pump-probe spectra. DFT/MRCI results and detailed water behaviour analysis. Bands assignation with TD-DFT NTO and RASPT2 orbitals See DOI: 10.1039/x0xx00000x

In this context, it is generally considered sufficient to locate crucial critical points on the PES such as excited state minima, conical intersections and avoided crossing, or minimum energy crossing points between states of different spin multiplicity. In turn, all the previous points may be related to the prediction of radiative (fluorescence and phosphorescence) or non-radiative (internal conversion, intersystem crossing, photochemical reactivity) phenomena. However, in several cases, the necessity to go beyond a purely static description of the PES is crucial to achieve a good comprehension of photophysics, especially when taking place in complex environments such as biological media.[25,26] Indeed, not only the environment may dramatically alter the PES, but the coupling between the chromophore and the environment degrees of freedom (i.e. the dynamics effects) may open totally new photophysical pathways.[27–30] Furthermore, a dynamic description – especially in its non-adiabatic framework – may provide a one-to-one mapping[31] with time resolved spectroscopies in terms of spectral signatures, excited state life-times and in some cases quantum efficiency.[25]

It is also noteworthy that the solvent dynamics - or more generally environment reorganisation - in the excited state will, in many cases be of crucial importance in guiding the photophysics.[32–35] Most importantly, in many instances, and in particular in homogeneous solvents, the former reorganisation takes place in the ultrafast regime and is achieved in the first hundreds of femtosecond after the excitation. Hence, the precise interpretation of time-resolved spectroscopy signatures is frequently cumbersome, and the synergy with molecular modelling is generally required. When the complexity of the molecular system of interest increases, e.g. involving the coupling between different chromophores in a dynamic fashion, time-resolved two-dimensional electronic spectroscopy (2DES) has appeared to be the experimental approach of choice.[36–39] However, once again the extremely rich density of information contained in 2DES spectra makes their interpretation particularly difficult and hence the assistance of molecular modelling almost compulsory.[40–43]

In this theoretical contribution, we explore the early-time (<300fs) excited-state dynamics of solvated BP by employing an original hybrid quantum mechanics/ molecular mechanics (QM/MM) approach based on time-dependent density functional theory (TD-DFT), in order to predict the ultrafast time-resolved spectroscopic signatures of BP in water. We exploit the results of the simulations to predict in particular UV-Vis transient absorption (TA) spectra as well as 2DES data. We assess the accuracy of this approach by (i) bench marking with high-level, computationally very expensive, modelling[44] and (ii) by comparing with experimental TA data obtained for BP in methanol, which has a similar polarity but weaker H-bonding character as compared to water, and where BP is much more soluble. While the predicted dominant spectral features match with the experimentally observed ones, our theoretical results anticipate an ultrafast spectral relaxation of the surrounding water molecules and may be interpreted in terms of relaxation of the solvent H-bonding interactions with BP in the excited state.

Material and Methods

Spectroscopic Measurements

Benzophenone (BP), and solvents from Sigma-Aldrich were used without further purification. The molar extinction coefficients were determined using a UV/Vis Perkin Elmer Lambda 950 spectrophotometer, adopting a 10-mm quartz cell and after solubilizing a precise amount of benzophenone in the various solvents. The ultrafast pump-probe setup (PP) was previously described elsewhere.[45–47] In short, a commercial optical parametric amplifier (OPA, "TOPAS" by Light Conversion), pumped by a Ti:Sa amplified laser system (Amplitude Technology, generating 40-fs, 800nm pulses at 5kHz) is used to produce a pump pulse at 333nm by 4th harmonic generation of the OPA signal beam, in order to excite BP its first electronic excited states. A white light pulse, obtained by supercontinum generation in CaF2, is used as a probe covering the 330-650nm spectral window. The experimental time resolution is ~ 60 fs, limited by the pump pulse spectral width. The pump and the probe beam polarisations were set at the magic angle (54.7°) to measure population kinetics under isotropic conditions. The differential absorption spectra (ΔA) spectra were corrected from the chirp of the probe beam, characterised by the time-dependence of the non-linear signal of the pure solvent. As a result, the zero time-delay is defined with an error bar of 20 fs throughout the covered spectral window.

Molecular Modelling and Simulation.

The ground state classical molecular dynamics (MD) of benzophenone (BP) in water was performed for a simulation time of 100 ns, using the Amber 16 suite of programs.[48] Water molecules were described by the TIP3P model,[49] while the Generalized Amber Force Field (GAFF)[50] and parm99 parameter sets were used to describe BP, including atomic charges assigned by the Restrained Electro-Static Potential (RESP) protocol,[51] as it was proven to be a suitable choice in previous work.[16] The overall system being neutral, no counterions were necessary. Details on parameters and pre-equilibration steps are given as Supplementary information.

Subsequently, a hybrid Quantum Mechanics/ Molecular Mechanics (QM/MM) MD was run on the ground state for 100 ps (time step: 0.5 fs), including BP in the QM region and describing it by Density Functional Theory (DFT). Especially, the CAM-B3LYP[52] functional and the 6-31G(d,p) basis set were used for the Gaussian09[53]/Cobramm[54] interface. This additional step was required in order to obtain more reliable BP snapshots together with accurate initial velocities to start QM/MM MDs on the lowest-excited singlet state (S_1). Indeed, 82 initial conditions were randomly selected from the ground state QM/MM MD to calculate the linear absorption spectrum. Moreover, on top of the selected snapshots, non-linear properties were calculated. More in detail, $S_1 \rightarrow S_0$ Stimulated Emission (SE) and $S_1 \rightarrow S_n$ Excited State Absorptions (ESAs) – including a total of 30 singlet states – were simulated, by

calculating all transition energies and transition dipole moments.

The same initial conditions were considered to run 82 QM/MM trajectories starting from the S_1 state, treating the QM region at Time Dependent-Density Functional Theory (TD-DFT) by the CAM-B3LYP[52] functional. The total simulation time was 300 fs (time step: 0.5 fs), not allowing surface-hops to other electronic states (*i.e.* under adiabatic conditions). Trajectories were stopped at 300 fs since we know that at this time already a considerable triplet population should be generated.[5] All snapshots at 100, 200 and 300 fs were extracted and their non-linear properties calculated as above explained for the 0 fs case. Compiling all the information, the pump-probe spectra and the 2-dimensional electronic spectra (2DES) were simulated (Figures 3 and 6).[42]

2DES spectra were simulated employing the sum-over-states (SOS) approach combined to a QM/MM scheme (SOS//QM/MM),[42] and employing the snapshot approximation (for time delay >0).[41] Energy levels and transition dipole moments were extracted and used to compute the non-linear responses as implemented in the Spectron 2.7 program.[55] Spectral lineshapes for each of the separate snapshots assume a pure dephasing in the Markovian approximation, being set to 1500 cm^{-1}. More accurate computational approaches have been recently developed to consider spectral diffusion and non-adiabatic effects on the simulated spectra,[56–61] yet these rely on more demanding schemes that are not currently feasible for the system under study. The inhomogeneous broadening of the signals is partially taken into account through the averaging over different geometrical conformations and water arrangements around the BP moiety.[62] Quasi-absorptive signals have been simulated with the collinear pump pulse pair condition (accounting for both rephasing and non-rephasing contributions simultaneously). All 2D spectra reported employ the all-parallel pulse polarisation configuration and are plotted on a linear scale. White light (infinite broadband) pulses are assumed, allowing us to observe the overall most intense signals throughout the 2D maps explored. Both ground state bleaching (GSB) and SE contributions appear as negative (blue) peaks, whereas ESAs appear as positive (red) peaks in the 2D spectra.

All single point calculations for linear and non-linear properties were carried out at B3LYP[63,64]/MM and CAM-B3LYP/MM levels of theory, using the TeraChem[65,66]/Amber interface. In order to assure a proper description of the solvent relaxation effects and to avoid wavefunction overpolarisation we systematically included in the QM partition BP as well as all the water molecules having a distance of less than 3 Å from the carbonyl oxygen. B3LYP functional provides excitation energy values in general good agreement with the multiconfigurational restricted active space second-order perturbation theory (RASPT2) methods with maximum energy differences of about 0.2 eV for all the states with the exception of S_4 that is red-shifted by about 0.4 eV. This behavior is reversed in the case of CAM-B3LYP that while it provides a good agreement for the S_4 state (0.06 eV) strongly deteriorates the description of the other states. Hence in order to have a balanced description of the electronic states, when using B3LYP functional the energy of the S_4 state obtained at TD-DFT level has been consistently shifted by 0.4 eV in order to correct the error of the hybrid functional in the description of this state and obtain results coherent with the multireference perturbation theory. It is also noteworthy that the calibration performed at multiconfigurational level shows a good agreement with the results obtained by Sergentu et al.[6]. However, and coherently with what previously observed[6] the increasing of static correlation via the RASPT2 formalisms induces a red shift of about 0.3 eV for S_1 and S_4 state.[44] For comparison purposes, the multiconfigurational Second-Order Perturbation Theory Restricted Active Space (RASPT2)[67] method was applied to compute linear and 2DES spectra at 0, 100, 200 and 300 fs for one representative trajectory. Due to the high computational time required for RASPT2 calculations, a comparison between TD-DFT and RASPT2 including several trajectories is not computationally feasible. Details on the RASPT2 calculations are given in the Supplementary information.

At TD-DFT level, in all cases the nature of the excited states has been characterised using the Natural Transition Orbital (NTO) formalism.[68–71] NTOs were obtained using NancyEX, a locally developed code.[69–71]

In addition and to account for the influence of double excitations excited states were also modelled using the DFT/MRCI approach.[72] In this case, for the DFT part, the BH-LYP functional in Turbomole 7.1[73,74] was used in combination with the TZVP basis set.[75] Multireference computations were carried out using the newly developed DFT/MRCI Hamiltonian by Lyskov et al.[76]

Results and Discussion

As a preliminary step, the steady-state spectra of solvated BP obtained experimentally and theoretically are presented in Figure 1. They feature a relatively strong absorption in the UV region (~ 290 nm) with tails extended in the UVA region (up to 370 nm). As expected and as confirmed by a number of theoretical calculations,[5,6] the UV maximum corresponds to the transition to the bright quasi-degenerate S_2/S_3 states, while the tail is due to the transition to S_1. On the other hand, the even stronger absorption in the farther UV region (250 nm) is mainly due to the transition to the higher S_4 state. The Natural Transition Orbitals (NTOs) for the two lowest states are reported in Figure 1c and one can easily recognize a π–π^* transition for S_2 and an n-π^* character, partially mixed with π–π^*, for S_1. Although π–π^* transitions are much brighter than the n-π^* one, their absorption maxima fall into too short wavelengths to be of practical importance on photosensitization processes, hence the study of the photophysics taking place from S_1 is by far more significant. The reproduction of the experimental spectrum by TD-DFT methods is accurate, especially when one takes into accounts the vibrational and dynamic effects by sampling the ground state conformational space via classic molecular dynamics, followed by QM/MM calculations of a set of snapshots, to

account for environmental effects. It is also noteworthy that other approaches such as DFT/multi-reference configuration interactions (DFT/MRCI) also yields a very good agreement with the experimental steady state spectrum as reported in ESI.

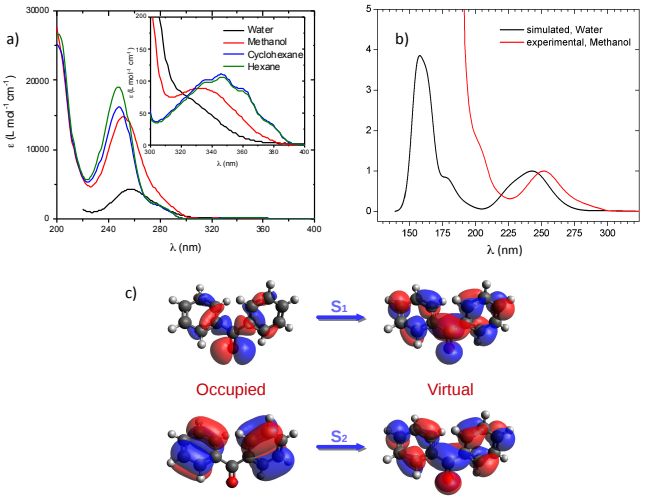

Figure 1. Experimental (a) and simulated (TD-DFT B3LYP) (b) steady state spectrum of benzophenone in various solvents. NTOs for the two lowest energy transitions are also presented (c).

As reported elsewhere[44] it is also remarkable that TD-DFT, especially using the B3LYP functional, provides a good and balanced description of the various excited states as compared to wave function based RASPT2 results.[44]

Experimental UV-Vis transient absorption (TA) spectra are reported in Figure 2 and SI. As expected and due to the almost dark S_1-S_0 transition the spectrum is dominated by excited state absorption (ESA) giving positive signals. When exciting to S_1 state (333 nm) in methanol, a broad band spanning from 520 to 590 nm dominates the early-time UV-Vis TA spectra. The data at 100 fs show two peaks at 520 and 580 nm, which sharpen around the 580nm band for longer delays (see the 300fs spectrum). As previously reported in different solvents[9–11,77] subsequent time evolution also occurs in methanol (see SI Fig S1) on the 10ps time scale and reveals the decay of this initial band and formation of a more intense, broader band, peaking at 520 nm, attributed to a triplet state formation. The later assignment is supported by previous non-adiabatic gas-phase simulations predicting a population of T1 and T2 with characteristic time constants τ of 1.0 and 4.5 ps, respectively.[5]

The experimental results obtained in hexane (see SI Fig S1) yields almost indistinguishable features as compared to methanol, indicating no effect of solvent polarity.

The simulated pump-probe spectra obtained by explicitly propagating BP in water solution on the S_1 potential energy surface through QM/MM for a statistical ensemble of starting conformations are presented in Figure 2. DFT/MRCI results have also been obtained for the time resolved simulated spectra and are in qualitative agreement with the TD-DFT results. The early TA spectral signature, i.e. prior to the intersystem crossing and triplet population, is very well reproduced, with the expected ESA band at around 15000-20000 cm^{-1} (560 nm).

Figure 2. Simulated (TD-DFT B3LYP) pump-probe spectra of BP in water solution in cm^{-1} scale at three different (100, 200, and 300 fs) delay times. The environment is taken explicitly into accounts via QM/MM calculations performed on top of the snapshots extracted from the molecular dynamic trajectories. Experimental pump-probe spectra for BP in methanol are reported for a direct

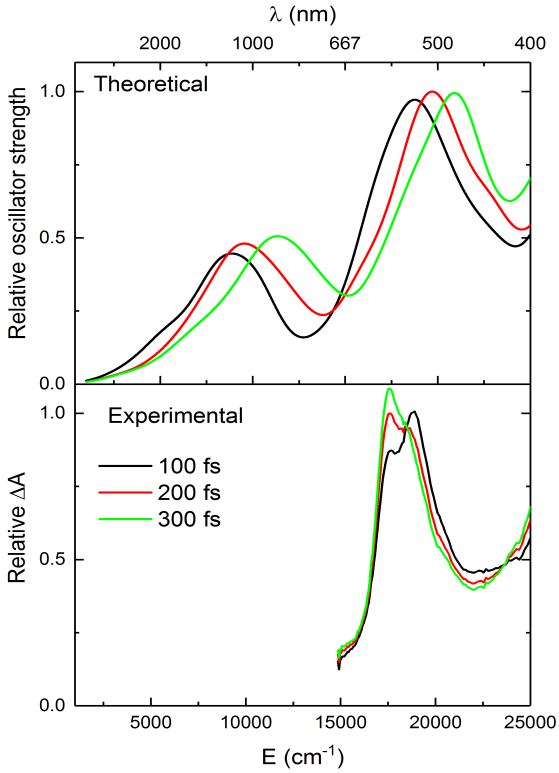

comparison. The relative intensities have been normalised to facilitate the comparison.

This bright band can be assigned to transitions taking place from S_1 to relatively high-energy states. As also shown in a previous contribution[44] the transitions involves the π* system of the aromatic ring and the excited n level of the carbonyl oxygen. However, while the experimental spectrum in methanol presents a slight red shift most likely attributable to intramolecular vibrational relaxation, the simulated results in water show a significant blue-shift of about 4000 cm^{-1} (0.5 eV) from 100 to 300 fs. In addition we also predict another ESA band at longer wavelengths (880-1500 nm), i.e. outside the present experimental probing window, which is also blue-shifting by about 4000 cm^{-1} in the first 300 fs. The analysis of the NTOs involved allows characterizing this low-energy band as mainly due to $S_1 \rightarrow S_3$ and $S_1 \rightarrow S_4$ transitions. The predicted, important blue shift of the ESA over the first 300fs, both in the visible and in the infrared region, is indicative of a rather important stabilisation of the S_1 state upon reorganisation of the environment. Indeed, when analysing the *ab-initio* QM/MM MD performed on the S_1 potential energy surface we notice a rather important reorganisation of the solvent H-bonding network around the carbonyl functional group (Figure 3).Consistently with the increased basicity of BP in the n-π* S_1

state, we observe a strong reinforcement of the hydrogen bonding with water molecules. In particular, in some of the trajectories we observe the accumulation of 4 or 5 water molecules at a distance from the carbonyl oxygen that is compatible with the formation of hydrogen bonds or a strong electrostatic interaction (3 Å). Most interestingly, according to our simulations this reorganisation takes place extremely rapidly as observed in Figure 3c.

The important effect of the water field reorganisation in promoting S_1 stabilisation and hence the ESA blue-shifting can also explain the difference in the experimental results. Indeed due to solubility issues, pump-probe spectra were performed in methanol, i.e. a less protic solvent than water, where no such blue-shift is observed. We note that already the steady state spectra of BP in methanol and water are different (see Figure 1a inset), already pointing to a significant difference between water and methanol regarding the solvent influence on BP. In particular due to the less pronounced protic nature, and hydrogen bond strength of methanol we expect a slightly weaker effect of the relaxation, which is coherent with the negligible spectral shift observed experimentally.

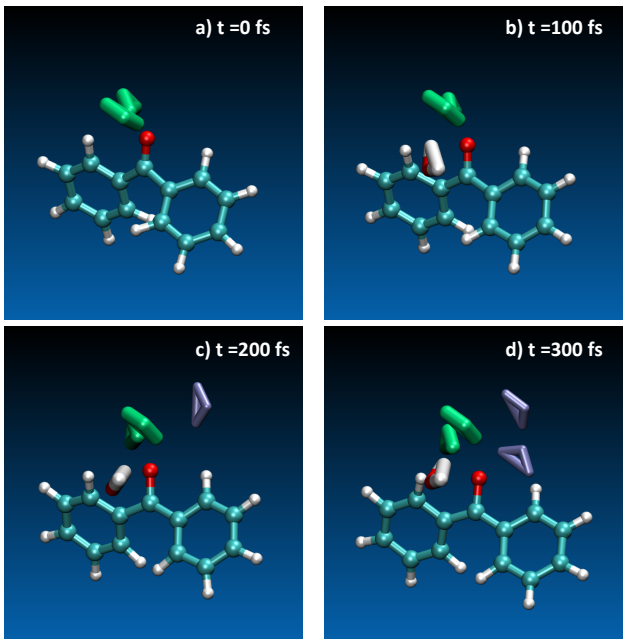

Figure 3. Snapshots from a representative QM/MM MD trajectory showing the solvent network reorganisation in the excited state. Water molecules in light green were already interacting in the ground state and stay persistently in the vicinity of the carbonyl oxygen in the excited state. The water molecule in element type colours forms a new hydrogen bond in the excited state, while the mauve coloured one forms less stable interactions

Interestingly enough, we note a different behaviour of the different water molecules. In particular, we evidence the formation of a very strong hydrogen bond with one water molecule in between 100 and 200 fs. As indicated in Figure 4 the formation of this hydrogen bonding is strongly coupled with the vibrational cooling of the excited carbonyl C=O distance. Indeed from 0 up to 150 fs we observe large amplitudes of the CO vibrations while the water molecule is rapidly approaching BP. Subsequently one observes a large plateau in which water persistently resides close to BP and the carbonyl vibrations are strongly reduced. The correlation of the solvent relaxation with the vibrational cooling is also in line with the computed blue-shift of the ESA band due to the stabilization of the S_1 state.

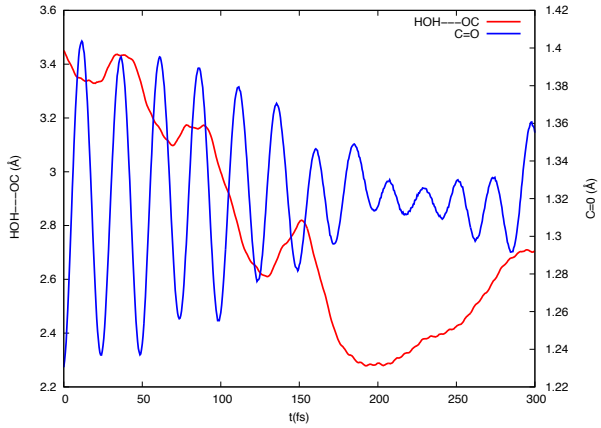

Figure 4. Time series of the distance between O(BP) atom and the water molecule hydrogen forming the new H-bond in the excited state. The carbonyl C=O bond length is also reported showing the correlation with the vibrational relaxation of the excitation. The considered water molecule is the one reproduced in element type colours in Figure 3.

Beyond (1D) transient absorption spectroscopy, we also simulated (using the same statistical ensemble of trajectories) the time-resolved 2D electronic spectrum (2DES) at TD-DFT level (Figure 5). More specifically we report 2D spectra in the spectral region associated to UV pumping (i.e. in the S_1 state) and Vis probing, i.e. the region where the most intense S_1-ESA signals are expected. The 2D-UV/Vis spectrum at time-zero shows the presence of an intense ESA band at $\Omega_1 \approx 31000$ cm^{-1} and $\Omega_3 \approx 17000$ cm^{-1}, rather symmetric (along Ω_3) with two less bright satellite signals at $\Omega_3 \approx 13000$ cm^{-1} and $\Omega_3 = 23000$ cm^{-1}. At longer times the main band experiences an important broadening along Ω_3, already evident at 100 fs. At the same time, the 2D-UV/Vis spectrum at 100 fs shows the appearance of line broadening along Ω_1 towards the red, consistently with the S_1 state stabilization. Notably, this is a spectral feature that cannot be appreciated in the 1D pump-probe spectra. At longer times, both Ω_1 and Ω_3 broadenings increase as the vibrational cooling and solvent relaxation occur. It is necessary to mention that these are lower bound estimates of line broadenings, as a single configuration of solvent surrounding molecules is considered for each snapshot analysed and other approximations are in place (see Material and Methods). As observed in simulated pump-probe spectra, an overall blue shift of all the ESA signals is also present in the 2D spectra. In order to evaluate the accuracy of the reported TD-DFT bidimensional spectra, we have computed the nonlinear spectra at the RASPT2 level.[78] Given the extremely high computational cost of such approach, the spectra simulations have been limited to a single trajectory (i.e. one snapshot for each time delay), as reported in the SI (Figure S3), showing an

acceptable agreement between B3LYP and RASPT2 spectra, despite the fact that relative signal intensities and transition energies might be significantly affected by double-excitations contributions accounted for only with the multiconfigurational treatment.

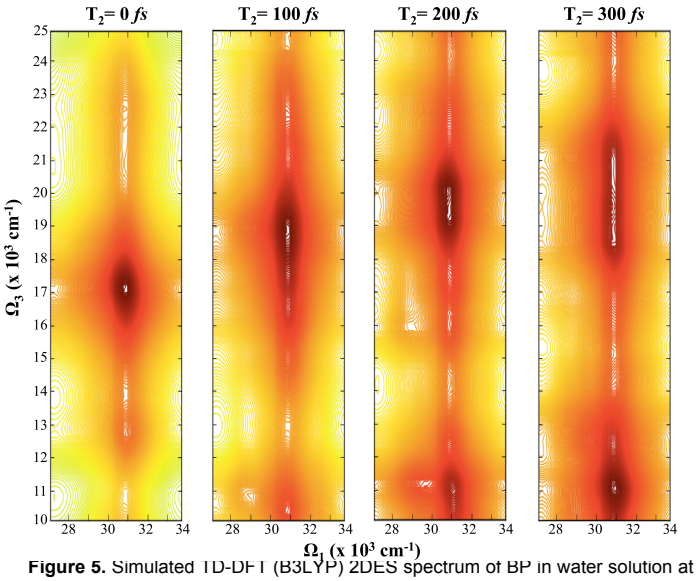

Figure 5. Simulated TD-DFT (B3LYP) 2DES spectrum of BP in water solution at 0, 100, 200 and 300 fs. Ω_1 and Ω_3 refer to pump and probe frequencies, respectively.

Conclusions

We have reported a systematic study of the ultrafast spectroscopic response of the paradigmatic sensitizer benzophenone. In particular we have developed a theoretical approach allowing us to model the spectroscopic signatures of BP in solution, at a level that enables direct comparison with experimental time-resolved spectroscopy data.

Our simulations highlight important time-dependent evolution of the low-energy (IR) ESA bands, which is specifically attributed to the evolution of the solvent H-bonding network around the BP carbonyl moiety. Most specifically the coupling between the vibrational relaxation of the elongated CO bond and the ultrafast formation of a new persistent hydrogen bond with solvent water molecules has been predicted. In addition, the first 2DES spectrum of BP in water taking into account the vibrational and dynamical broadening and time evolution has been simulated at TD-DFT level. The global features of the latter seem to confirm the important role of the water solvent dynamics. Even though, the experimental results have been available only in methanol, due to solubility issue, the role of the solvent relaxation is confirmed, even if its magnitude is less important. Our work allows shedding a new light on the complex photophysics of benzophenone in water environment and on the important role played by H-bonding network relaxation. At the same time it constitutes a very important proof of concept of the powerful possibilities offered by the combining use of multiscale modelling and simulation and time-resolved spectroscopy.

Conflicts of interest

There are no conflicts to declare.

Acknowledgements

Supports from Universities of Lorraine and Strasbourg, as well as ENS Lyon and CNRS are gratefully acknowledged. The present work was funded under the French National Agency (ANR) grant “Femto-2DNA” project (ANR-15-CE29-0010-01), and Labex NIE (ANR-11-LABX-0058_NIE). I.R. gratefully acknowledges the support of ENSL “Fonds Recherche, MI-LOURD-FR15” and the PSMN for computing time.

Authors’ Contribution

EZ, MM, J.S-M. O.W. performed the molecular modelling, J.B. registered the spectra, M.G., A.N., and O.W. developed the computational codes used. A.M. planned the study and wrote most of the manuscript. All the authors discussed the results and participated in the manuscript preparation.

Notes and references

1 M. C. Cuquerella, V. Lhiaubet-Vallet, J. Cadet and M. A. Miranda, Benzophenone photosensitized DNA damage, *Acc. Chem. Res.*, 2012, **45**, 1558–1570.

2 M. Sugiura, R. Hayakawa, Z. Xie, K. Sugiura, K. Hiramoto and M. Shamoto, Experimental study on phototoxicity and the photosensitization potential of ketoprofen, suprofen, tiaprofenic acid and benzophenone and cross-reactivity in guinea pigs, *Photoderm Photoimmunol Photomed.*, 2002, **18**, 82–89.

3 Y. Matsushita, Y. Kajii and K. Obi, Photochemical Reaction of Excited Benzophenone in the Gas Phase, *J. Phys. Chem.*, 1992, **96**, 4455–4458.

4 S. Yabumoto, S. Sato and H. Hamaguchi, Vibrational and electronic infrared absorption spectra of benzophenone in the lowest excited triplet state, *Chem. Phys. Lett.*, 2005, **416**, 100–103.

5 M. Marazzi, S. Mai, D. Roca-Sanjuán, M. G. Delcey, R. Lindh, L. González and A. Monari, Benzophenone Ultrafast Triplet Population: Revisiting the Kinetic Model by Surface-Hopping Dynamics, *J. Phys. Chem. Lett.*, 2016, **7**, 622–626.

6 D.-C. Sergentu, R. Maurice, R. W. A. Havenith, R. Broer and D. Roca-Sanjuán, Computational determination of the dominant triplet population mechanism in photoexcited benzophenone, *Phys. Chem. Chem. Phys.*, 2014, **16**, 25393–25403.

7 L. Favero, G. Granucci and M. Persico, Surface hopping investigation of benzophenone excited state dynamics, *Phys. Chem. Chem. Phys.*, 2016, **18**, 10499–10506.

8 K. K. Chin, A. Natarajan, M. N. Gard, L. M. Campos, H. Shepherd, E. Johansson and M. A. Garcia-Garibay, Pump-probe spectroscopy and circular dichroism of nanocrystalline benzophenone--towards absolute kinetic measurements in solid state photochemical reactions., *Chem. Commun. (Camb).*, 2007, 4266–4268.

9 B. K. Shah, M. A. J. Rodgers and D. C. Neckers, The S2 ,Üí S1 Internal Conversion of Benzophenone and p-Iodobenzophenone1, *J. Phys. Chem. A*, 2004, **108**, 6087–6089.

10 S. Aloïse, C. Ruckebusch, L. Blanchet, J. Réhault, G. Buntinx and J. P. Huvenne, The benzophenone S1(n,π*) →T1(n,π *) states intersystem crossing reinvestigated by ultrafast absorption spectroscopy and multivariate curve resolution, *J. Phys. Chem. A*, 2008, **112**, 224–231.

11 N. Tamai, T. Asahi and H. Masuhara, Intersystem crossing of benzophenone by femtosecond transient grating spectroscopy, *Chem. Phys. Lett.*, 1992, **198**, 413–418.

12 G. Spighi, M.-A. Gaveau, J.-M. Mestdagh, L. Poisson and B. Soep, Gas phase dynamics of triplet formation in benzophenone, *Phys. Chem. Chem. Phys.*, 2014, **16**, 9610–9618.

13 B. Soep, J.-M. Mestdagh, M. Briant, M.-A. Gaveau and L. Poisson, Direct observation of slow intersystem crossing in an aromatic ketone, fluorenone, *Phys. Chem. Chem. Phys.*, 2016, **18**, 22914–22920.

14 L. Pastor-Pérez, E. Barriau, H. Frey, J. Pérez-Prieto and S. E. Stiriba, Photocatalysis within hyperbranched polyethers with a benzophenone core, *J. Org. Chem.*, 2008, **73**, 4680–4683.

15 V. Singh and P. Das, Condensation of DNA-A putative obstruction for repair process in abasic clustered DNA damage, *DNA Repair (Amst).*, 2013, **12**, 450–457.

16 E. Dumont and A. Monari, Benzophenone and DNA: Evidence for a double insertion mode and its spectral signature, *J. Phys. Chem. Lett.*, 2013, **4**, 4119–4124.

17 H. Gattuso, E. Dumont, C. Chipot, A. Monari and F. Dehez, Thermodynamics of DNA: sensitizer recognition. Characterizing binding motifs with all-atom simulations, *Phys. Chem. Chem. Phys.*, 2016, **18**, 33180–33186.

18 E. Dumont, M. Wibowo, D. Roca-Sanjuán, M. Garavelli, X. Assfeld and A. Monari, Resolving the benzophenone DNA-photosensitization mechanism at QM/MM level, *J. Phys. Chem. Lett.*, 2015, **6**, 576–580.

19 M. Marazzi, M. Wibowo, H. Gattuso, E. Dumont, D. Roca-Sanjuán and A. Monari, Hydrogen abstraction by photoexcited benzophenone: consequences for DNA photosensitization, *Phys. Chem. Chem. Phys.*, 2016, **18**, 7829–7836.

20 R. Szabla, J. Campos, J. E. Sponer, J. Sponer, R. W. Gora and J. D. Sutherland, Excited-state hydrogen atom abstraction initiates the photochemistry of [beta]-2[prime or minute]-deoxycytidine, *Chem. Sci.*, 2015, 2035–2043.

21 M. De Li, T. Su, J. Ma, M. Liu, H. Liu, X. Li and D. L. Phillips, Phototriggered release of a leaving group in Ketoprofen derivatives via a benzylic carbanion pathway, but not via a biradical pathway, *Chem. - A Eur. J.*, 2013, **19**, 11241–11250.

22 L. L. Costanzo, G. De Guidi, G. Condorelli, A. Cambria and M. Fama, Molecular mechanism of drug photosensitization II. Photoemolysis sensitized by ketoprofen, *Photochem. Photobiol.*, 1989, **50**, 359–365.

23 E. Bignon, M. Marazzi, V. Besancenot, H. Gattuso, G. Drouot, C. Morell, L. A. Eriksson, S. Grandemange, E. Dumont and A. Monari, Ibuprofen and ketoprofen potentiate UVA-induced cell death by a photosensitization process, *Sci. Rep.*, 2017, **7**, 8885.

24 Y.-J. Liu, D. Roca-Sanjuan and R. Lindh, *Computational Photochemistry and Photophysics: the state of the art*, 2012, vol. 40.

25 D. Polli, P. Altoè, O. Weingart, K. M. Spillane, C. Manzoni, D. Brida, G. Tomasello, G. Orlandi, P. Kukura, R. A. Mathies, M. Garavelli and G. Cerullo, Conical intersection dynamics of the primary photoisomerization event in vision, *Nature*, 2010, **467**, 440–443.

26 M. Manathunga, X. Yang, H. L. Luk, S. Gozem, L. M. Frutos, A. Valentini, N. Ferrè and M. Olivucci, Probing the Photodynamics of Rhodopsins with Reduced Retinal Chromophores, *J. Chem. Theory Comput.*, 2016, **12**, 839–850.

27 J. J. Nogueira, M. Oppel and L. González, Enhancing intersystem crossing in phenotiazinium dyes by intercalation into DNA, *Angew. Chemie - Int. Ed.*, 2015, **54**, 4375–4378.

28 J. J. Nogueira, M. Meixner, M. Bittermann and L. González, Impact of Lipid Environment on Photodamage Activation of Methylene Blue, *ChemPhotoChem*, 2017, **1**, 178–182.

29 K. Hirakawa and T. Hirano, The Microenvironment of DNA Switches the Activity of Singlet Oxygen Generation Photosensitized by Berberine and Palmatine, *Photochem. Photobiol.*, 2008, **84**, 202–208.

30 E. Dumont and A. Monari, Interaction of Palmatine with {DNA}: An Environmentally Controlled Phototherapy Drug, *J. Phys. Chem. B*, 2015, **119**, 410–419.

31 A. S. Petit and J. E. Subotnik, Calculating time-resolved differential absorbance spectra for ultrafast pump-probe experiments with surface hopping trajectories, *J. Chem. Phys.*, 2014, **141**, 154108.

32 F. Messina, O. Bräm, A. Cannizzo and M. Chergui, Real-time observation of the charge transfer to solvent dynamics, *Nat. Commun.*, 2013, **4**, 2119.

33 T. Polívka and V. Sundström, Ultrafast dynamics of carotenoid excited states-from solution to natural and artificial systems, *Chem. Rev.*, 2004, **104**, 2021–2071.

34 H. a Frank, J. a Bautista, J. Josue, Z. Pendon, R. G. Hiller, F. P. Sharples, D. Gosztola and M. R. Wasielewski, Effect of the Solvent Environment on the Spectroscopic Properties and Dynamics of the Lowest Excited States of Carotenoids, *J. Phys. Chem. B*, 2000, **104**, 4569–4577.

35 N. H. Damrauer, Femtosecond Dynamics of Excited-State Evolution in [Ru(bpy)3]2+, *Science (80-.).*, 1997, **275**, 54–57.

36 J. D. Hybl, A. W. Albrecht, S. M. Gallagher Faeder and D. M. Jonas, Two-dimensional electronic spectroscopy, *Chem.*

Phys. Lett., 1998, **297**, 307–313.

37 B. A. West and A. M. Moran, Two-dimensional electronic spectroscopy in the ultraviolet wavelength range, *J. Phys. Chem. Lett.*, 2012, **3**, 2575–2581.

38 M. Maiuri, J. Réhault, A. M. Carey, K. Hacking, M. Garavelli, L. Lüer, D. Polli, R. J. Cogdell and G. Cerullo, Ultra-broadband 2D electronic spectroscopy of carotenoid-bacteriochlorophyll interactions in the LH1 complex of a purple bacterium, *J. Chem. Phys.*, 2015, **142**, 212433.

39 Q. Li, A. Giussani, J. Segarra-Martí, A. Nenov, I. Rivalta, A. A. Voityuk, S. Mukamel, D. Roca-Sanjuán, M. Garavelli and L. Blancafort, Multiple Decay Mechanisms and 2D-UV Spectroscopic Fingerprints of Singlet Excited Solvated Adenine-Uracil Monophosphate, *Chem. - A Eur. J.*, 2016, **22**, 7497–7507.

40 A. Nenov, J. Segarra-Martí, A. Giussani, I. Conti, I. Rivalta, E. Dumont, V. K. Jaiswal, S. F. Altavilla, S. Mukamel and M. Garavelli, Probing deactivation pathways of DNA nucleobases by two-dimensional electronic spectroscopy: first principles simulations, *Faraday Discuss.*, 2015, **177**, 345–362.

41 I. Rivalta, A. Nenov, O. Weingart, G. Cerullo, M. Garavelli and S. Mukamel, Modelling time-resolved two-dimensional electronic spectroscopy of the primary photoisomerization event in rhodopsin, *J. Phys. Chem. B*, 2014, **118**, 8396–8405.

42 I. Rivalta, A. Nenov, G. Cerullo, S. Mukamel and M. Garavelli, *Int. J. Quantum Chem.*, 2014, 114, 85–93.

43 A. Nenov, I. Rivalta, G. Cerullo, S. Mukamel and M. Garavelli, Disentangling peptide configurations via two-dimensional electronic spectroscopy: Ab initio simulations beyond the Frenkel exciton hamiltonian, *J. Phys. Chem. Lett.*, 2014, **5**, 767–771.

44 J. Segarra-Martí, E. Zvereva, M. Marazzi, J. Brazard, E. Dumont, X. Assfeld, S. Haacke, M. Garavelli, A. Monari, J. Léonard and I. Rivalta, Resolving the singlet excited states manifold of benzophenone by first-principles and ultrafast electronic spectroscopy, *J. Chem. Theory Comput.*, 2017, submitted.

45 J. Briand, O. Bräm, J. Réhault, J. Léonard, A. Cannizzo, M. Chergui, V. Zanirato, M. Olivucci, J. Helbing and S. Haacke, Coherent ultrafast torsional motion and isomerization of a biomimetic dipolar photoswitch., *Phys. Chem. Chem. Phys.*, 2010, **12**, 3178–87.

46 T. Roland, J. Léonard, G. Hernandez Ramirez, S. Méry, O. Yurchenko, S. Ludwigs and S. Haacke, Sub-100 fs charge transfer in a novel donor–acceptor–donor triad organized in a smectic film, *Phys. Chem. Chem. Phys.*, 2012, **14**, 273–279.

47 M. Paolino, M. Gueye, E. Pieri, M. Manathunga, S. Fusi, A. Cappelli, L. Latterini, D. Pannacci, M. Filatov, J. Léonard and M. Olivucci, Design, Synthesis, and Dynamics of a Green Fluorescent Protein Fluorophore Mimic with an Ultrafast Switching Function, *J. Am. Chem. Soc.*, 2016, **138**, 9807–9825.

48 D. A. Case, T. E. Cheatham, T. Darden, H. Gohlke, R. Luo, K. M. Merz, A. Onufriev, C. Simmerling, B. Wang and R. J. Woods, *J. Comput. Chem.*, 2005, 26, 1668–1688.

49 P. Mark and L. Nilsson, Structure and dynamics of the TIP3P, SPC, and SPC/E water models at 298 K, *J. Phys. Chem. A*, 2001, **105**, 9954–9960.

50 J. Wang, R. M. Wolf, J. W. Caldwell, P. A. Kollman and D. A. Case, Development and testing of a general Amber force field, *J. Comput. Chem.*, 2004, **25**, 1157–1174.

51 J. Wang, P. Cieplak and P. A. Kollman, How well does a restrained electrostatic potential (RESP) model perform in calculating conformational energies of organic and biological molecules?, *J. Comput. Chem.*, 2000, **21**, 1049–1074.

52 T. Yanai, D. P. Tew and N. C. Handy, A new hybrid exchange-correlation functional using the Coulomb-attenuating method (CAM-B3LYP), *Chem. Phys. Lett.*, 2004, **393**, 51–57.

53 D. J. Frisch, M. J.; Trucks, G.W.; Schlegel, H. B.; Scuseria, G. E.; Robb, M. A.; Cheeseman, J. R.; Scalmani, G.; Barone, V.;Mennucci, B.; Petersson, G. A.; Nakatsuji, H.; Caricato, M.; Li, X.; Hratchian, H. P.; Izmaylov, A. F.; Bloino, J.; Zheng, G.; Sonnenber, Gaussian 09, *Gaussian, Inc. Wallingford CT*, 2009, 2–3.

54 P. Altoè, M. Stenta, A. Bottoni, M. Garavelli, G. Maroulis and T. E. Simos, in *AIP Conference Proceedings*, AIP, 2007, vol. 963, pp. 491–505.

55 S. Mukamel, R. Oszwaldowski and D. Abramavicius, Sum-over-states versus quasiparticle pictures of coherent correlation spectroscopy of excitons in semiconductors: Femtosecond analogs of multidimensional NMR, *Phys. Rev. B - Condens. Matter Mater. Phys.*, 2007, **75**, 245305.

56 D. Abramavicius, B. Palmieri, D. V. Voronine, F. Šanda and S. Mukamel, Coherent multidimensional optical spectroscopy of excitons in molecular aggregates; quasiparticle versus supermolecule perspectives, *Chem. Rev.*, 2009, **109**, 2350–2408.

57 A. Nenov, A. Giussani, B. P. Fingerhut, I. Rivalta, E. Dumont, S. Mukamel and M. Garavelli, Spectral lineshapes in nonlinear electronic spectroscopy, *Phys. Chem. Chem. Phys.*, 2015, **17**, 30925–30936.

58 M. Richter and B. P. Fingerhut, Simulation of multi-dimensional signals in the optical domain: Quantum-classical feedback in nonlinear exciton propagation, *J. Chem. Theory Comput.*, 2016, **12**, 3284–3294.

59 R. Tempelaar, C. P. Van Der Vegte, J. Knoester and T. L. C. Jansen, Surface hopping modeling of two-dimensional spectra, *J. Chem. Phys.*, 2013, **138**, 164106.

60 C. P. Van Der Vegte, A. G. Dijkstra, J. Knoester and T. L. C. Jansen, Calculating two-dimensional spectra with the mixed quantum-classical ehrenfest method, *J. Phys. Chem. A*, 2013, **117**, 5970–5980.

61 M. Kowalewski, B. P. Fingerhut and K. E. Dorfman, Simulating Coherent Multidimensional Spectroscopy of Nonadiabatic Molecular Processes ; from the Infrared to the X-ray Regime, *Chem. Rev.*, 2017, **117**, 1–211.

62 J. Segarra-Martí, V. K. Jaiswal, A. J. Pepino, A. Giussani, A. Nenov, S. Mukamel, M. Garavelli and I. Rivalta, Two-dimensional electronic spectroscopy as a tool for tracking

molecular conformations in DNA/RNA aggregates, *Faraday Discuss.*, , DOI:10.1039/C7FD00201G.
63 A. Becke, B3LYP, *J. Chem. Phys.*, 1993, **98**, 5648–5652.
64 P. J. Stephens, F. J. Devlin, C. F. Chabalowski and M. J. Frisch, Ab Initio Calculation of Vibrational Absorption and Circular Dichroism Spectra Using Density Functional Force Fields, *J. Phys. Chem.*, 1994, **98**, 11623–11627.
65 A. V. Titov, I. S. Ufimtsev, N. Luehr and T. J. Martinez, Generating efficient quantum chemistry codes for novel architectures, *J. Chem. Theory Comput.*, 2013, **9**, 213–221.
66 I. S. Ufimtsev and T. J. Martinez, Quantum chemistry on graphical processing units. 3. Analytical energy gradients, geometry optimization, and first principles molecular dynamics, *J. Chem. Theory Comput.*, 2009, **5**, 2619–2628.
67 V. Sauri, L. Serrano-andre, A. Rehaman and M. Shahi, Benchmark Study of the Multiconfigurational Second-Order Perturbation Theory Restricted Active Space (RASPT2) Method for Electronic Excited States, *J. Chem. Theory Comput.*, 2011, **7**, 153–168.
68 R. L. Martin, Natural transition orbitals, *J. Chem. Phys.*, 2003, **118**, 4775–4777.
69 T. Etienne, X. Assfeld and A. Monari, New insight into the topology of excited states through detachment/attachment density matrices-based centroids of charge, *J. Chem. Theory Comput.*, 2014, **10**, 3906–3914.
70 T. Etienne, X. Assfeld and A. Monari, Toward a quantitative assessment of electronic transitions" charge-transfer character, *J. Chem. Theory Comput.*, 2014, **10**, 3896–3905.
71 T. Etienne, Probing the locality of excited states with linear algebra, *J. Chem. Theory Comput.*, 2015, **11**, 1692–1699.
72 S. Grimme and M. Waletzke, A combination of Kohn–Sham density functional theory and multi-reference configuration interaction methods, *J. Chem. Phys.*, 1999, **111**, 5645–5655.
73 R. Ahlrichs, M. Bär, M. Häser, H. Horn and C. Kölmel, Electronic structure calculations on workstation computers: The program system turbomole, *Chem. Phys. Lett.*, 1989, **162**, 165–169.
74 Turbomole v7.1 2016, a development of university of Karlsruhe and Forschungszentrum Karlsruhe GmbH, 1989-2007, Turbomole GmbH, since 2007, http://www.turbomole.com.
75 A. Schäfer, C. Huber and R. Ahlrichs, Fully optimized contracted Gaussian basis sets of triple zeta valence quality for atoms Li to Kr, *J. Chem. Phys.*, 1994, **100**, 5829–5835.
76 I. Lyskov, M. Kleinschmidt and C. M. Marian, Redesign of the DFT/MRCI Hamiltonian, *J. Chem. Phys.*, 2016, **144**, 34104.
77 T. Merz, M. Wenninger, M. Weinberger, E. Riedle, H.-A. Wagenknecht and M. Schütz, Conformational control of benzophenone-sensitized charge transfer in dinucleotides, *Phys. Chem. Chem. Phys.*, 2013, **15**, 18607.
78 F. Aquilante, J. Autschbach, R. K. Carlson, L. F. Chibotaru, M. G. Delcey, L. De Vico, I. Fdez. Galván, N. Ferré, L. M. Frutos, L. Gagliardi, M. Garavelli, A. Giussani, C. E. Hoyer, G. Li Manni, H. Lischka, D. Ma, P. Å. Malmqvist, T. Müller, A. Nenov, M. Olivucci, T. B. Pedersen, D. Peng, F. Plasser, B. Pritchard, M. Reiher, I. Rivalta, I. Schapiro, J. Segarra-Martí, M. Stenrup, D. G. Truhlar, L. Ungur, A. Valentini, S. Vancoillie, V. Veryazov, V. P. Vysotskiy, O. Weingart, F. Zapata and R. Lindh, Molcas 8: New capabilities for multiconfigurational quantum chemical calculations across the periodic table, *J. Comput. Chem.*, 2016, **37**, 506–541.